NANO LETTERS

2005
Vol. 5, No. 1
131−135

Electrochemical Ostwald Ripening of Colloidal Ag Particles on Conductive Substrates

Peter L. Redmond, A. J. Hallock, and Louis E. Brus*

Chemistry Department, Columbia University, New York, New York 10027

Received October 29, 2004; Revised Manuscript Received November 18, 2004

ABSTRACT

Thermally evaporated silver nanoparticles on conducting substrates spontaneously evolve in size when immersed in pure water. The process was studied using scanning electron microscopy (SEM), energy-dispersive X-ray analysis (EDX), and optical absorption spectroscopy. The particles are proposed to reform through an electrochemical Ostwald ripening mechanism driven by the size dependence of the work function and standard electrode potential. We also discuss prior literature experiments where this process appears to occur. Our results show the sensitivity of the electrochemical properties of metallic nanoparticles at relatively large sizes (∼50 nm).

We report spontaneous morphological reformation of evaporated silver nanoparticles on indium tin oxide (ITO) and flat graphite (HOPG) surfaces in pure water. Over a period of hours at 23 °C, large faceted 100−300 nm crystallites grow as small 20 nm particles dissolve. This process does not appear to have been previously recognized. The mechanism is electrochemical Ostwald ripening driven by the particle size dependence of the Ag standard electrode potential and is facilitated by the high standard exchange rate of polycrystalline silver electrodes.[1]

Henglein and Plieth first explored the electrochemical properties of metal nanoparticles.[2−4] Plieth predicted a negative shift in the Ag standard electrode potential and decrease in the work function of small (<25 nm) metallic particles. The difference in standard electrode potentials causes differences in the equilibrium silver ion concentration around each particle. In our experiment Ag^+ ions move from small to large particles through the water, while electrons travel through the substrate. We unexpectedly observed this particle distribution coarsening in studies of Ag films intended for SERS studies.[5−9] The physical and photochemical properties of metallic particles and colloids have been recently reviewed.[10]

Silver metal thin films were thermally deposited under vacuum (10^{-6} Torr) onto polished fused quartz slides, indium tin oxide coated quartz slides ($R_s = 15 \pm 5\Omega$, Delta Technologies), and freshly cleaved highly oriented pyrolytic graphite (HOPG). The ∼1 cm^2 quartz and ITO substrates were cleaned by being sonicated in ethanol for 15 min, rinsed in acetone, and blown dry with N_2. Film thickness was evaluated during the evaporation by a calibrated frequency thickness monitor. Films were evaporated at a rate of 0.1 nm/s in an Edwards/BOC 306 thermal evaporator. Barnstead Nanopure water (σ > 17 MΩ/cm) was used to prepare all solutions. All chemicals used were reagent grade and used with out further purification. The films were stored under ambient conditions and were exposed to water by placing a drop of solution (> 1 mL) on the substrate. Sodium hydroxide and nitric acid were used to set the pH. Each sample was blown dry with N_2 after exposure to the solutions. SEM images were taken using a FEI XL SFEG instrument. EDX elemental analysis was carried out using a LEO 1443 attachment. Films coated onto quartz substrates were coated with 5 nm of Au before viewing to prevent charging during SEM imaging.

Figures 1A and 1D show initial SEM images of equivalent 1.5 nm and 15 nm thicknesses of Ag on HOPG. The thermal evaporation of 1.5 nm of Ag produces an array of ∼20 nm silver nanoparticles and 15 nm produces a broken thin film. When stored under ambient conditions, no change is observed. Upon exposure to pure water, the array of nanoparticles grows into larger faceted structures on the ITO and HOPG (Figures 1, 2). On the transparent ITO substrate, the color to the eye changes from dark purple to translucence as is evident from spectra in Figure 3. EDX elemental analysis on HOPG determined the faceted structures to be pure silver metal (error of <2 wt % for light elements). Thicker films (40, 60, 110, 200 nm) were also exposed to Nanopure water on HOPG and found to reform in the same way over longer time scales as shown in Figure 4. In contrast to this process on HOPG and ITO, no change was observed when a 5 nm thick film on quartz was exposed to water.

It is known that unpassivated silver nanoparticles slowly oxidize in ambient conditions.[11,12] As Ag^+ ion is soluble,

* Corresponding author. E-mail: leb26@columbia.edu.

10.1021/nl048204r CCC: $30.25 © 2005 American Chemical Society
Published on Web 12/04/2004

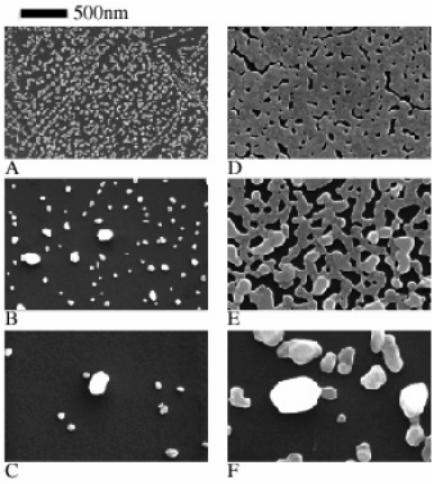

Figure 1. SEM images of evaporated Ag exposed to water on HOPG. Panels A, B, and C are of 1.5 nm of Ag with exposure times of 0 s, 100 s, and 7 h, respectively. Panels D, E, and F are of 15 nm of Ag with the same exposure times.

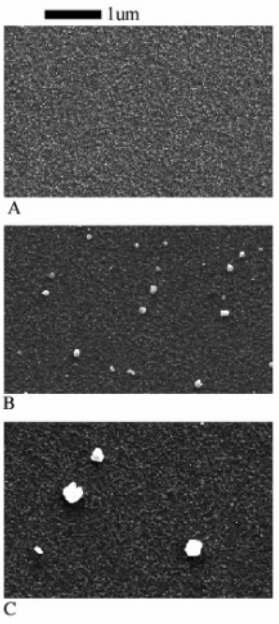

Figure 2. SEM images of Ag thermally evaporated onto ITO. Figures A, B, and C are of 1.5 nm of Ag with exposure times of 0 s, 1000 s, and 7 h, respectively. The intrinsic roughness of the ITO film is apparent in C.

we decided to check if the supposed oxidized component affects the growth process. The two-electrode system shown in Figure S1 (Supporting Information) was used to hold the films under a reducing potential while exposed to water. The films on ITO were attached to the negative side of the 1.5 V potential and a clean uncoated piece of ITO served as the counter electrode. Several drops of Nanopure water bridged the two electrodes. The films do not reform in this arrangement; no observable change occurred in SEM images. Thus oxidized Ag is tentatively implicated.

The dependence on oxidized Ag was explored in several ways. A solution of 10 mM $AgNO_3$ reformed the films more quickly than pure water, as can be seen in Figure S2B,C (Supporting Information). Films on quartz did not reform

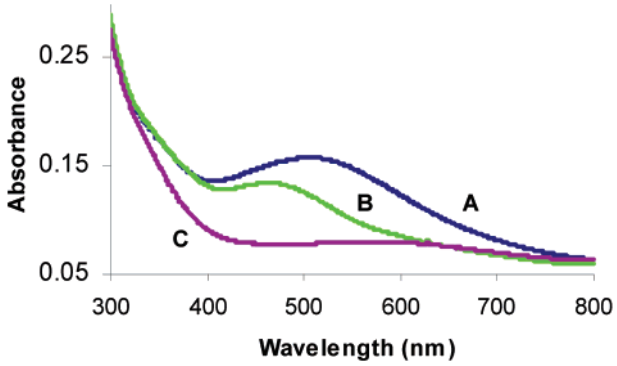

Figure 3. UV−vis absorption of the films pictured in Figure 2. Spectra A, B, and C are of 1.5 nm of Ag with exposure times of 0 s, 1000 s, and 7 h, respectively.

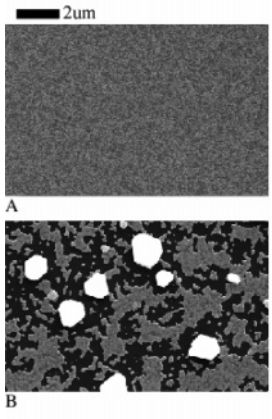

Figure 4. SEM images of a 60 nm film of Ag on HOPG: (A) before exposure to water; (B) after being exposed to water for 7 h.

with silver nitrate solution. A decrease in the reformation rate, compared to films exposed to pure water, occurred when films are exposed to a 10 mM solution of sodium nitrate (see Figure S2F,G). Since the solubility of Ag depends on pH, silver thin films were exposed to aqueous solutions of varying pH. Figures S3 and S4 (Supporting Information) show silver thin films exposed to pH 10 and pH 3 solutions. It was found that the basic solution inhibits the reformation while the acidic solution quickens the reaction. Silver thin films exposed to an aqueous 1% sodium citrate solution (by weight) are found not to reform, as is shown in Figure 5. As a final control experiment, films irradiated with 10 W/cm^2 of 514.5 nm, while being exposed to water, were found to reform at the same rate of silver films exposed to water in the dark.

The reduction of bulk silver is described by the half-cell reaction $Ag^+_{(aq)} + e^- \rightarrow Ag_{(s)}$ with $E^0_{bulk} = +0.80$ V versus NHE. According to Plieth, the standard electrode potential E^0_p of a small metal particle shifts negatively via the following equation, where γ is the surface tension, v_M is the molar volume, z is the lowest valence state, F is Faraday's constant, and r is the radius.

$$E^0_p = \left(E^0_{bulk} - \frac{2\gamma v_M}{zFr}\right) \quad (1)$$

Figure 6 shows a plot of the shift in the standard electrode

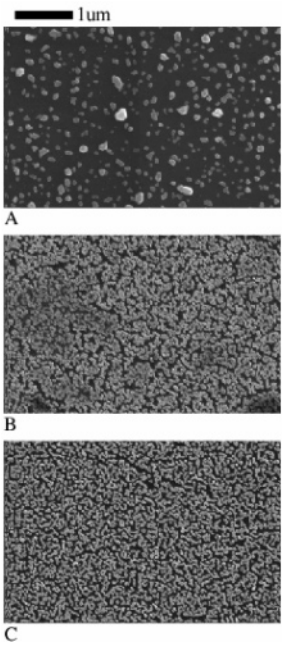

Figure 5. SEM images of 5 nm of Ag thermally evaporated onto HOPG. (A) 2 h exposure to pure water. (B) 2 h exposure to 1% citrate solution. (C) Control with no exposure.

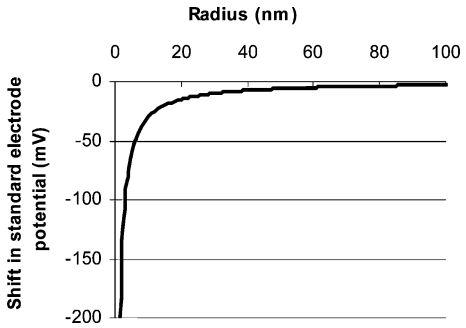

Figure 6. (A) Graph of the shift from bulk in standard electrode potential of small silver particles as described in eq 1, where $\gamma = 1.45$ J/m^2 is used as the surface tension of silver.[13]

potential of small silver particles as a function of radius.[13] A negative shift in the standard electrode potential of small particles means that smaller metal nanoparticles are more easily oxidized than bulk material. Such standard electrode potential shifts have been qualitatively studied for sizes less than 10 nm.[14,15] Similarly, the work function of small metal particles is depressed.[3]

In a heuristic sense, larger and smaller particles behave as different metals with different standard electrode potentials. If they are shorted to each other by a conductive substrate, then they function as cathode and anode in a galvanic cell when an electrolyte and reducible species (i.e., oxygen) are present. Thus reformulation is partially analogous to a microscopic surface corrosion cell.[16] Experimentally, the reaction does require a conducting substrate (it is not observed on quartz). The rate increases with the presence of silver nitrate in solution and does not occur in pure water if the particles are prevented from partially dissolving by the application of a reducing potential. Thus, the presence of some Ag^+ ion in solution is required.

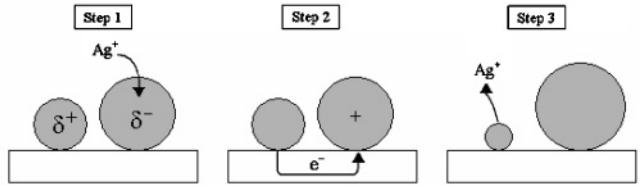

Figure 7. Diagram of the mechanism for the formation of faceted nanostructures from silver thin films is shown. The size difference resulting from the loss of a silver ion is greatly exaggerated.

In Figure 7, the larger particle has a partial negative charge and the smaller particle a partial positive charge at electrical equilibrium, due to the greater work function of the larger particle. Consequently, in solution there is an electric field drawing positive ions toward the larger particle. Furthermore, due to the standard electrode potential difference, the equilibrium concentration of Ag^+ ions near the larger particle is lower than near the smaller particle. Using standard thermodynamic arguments and taking the Ag^+ concentration to be at equilibrium with dissolved oxygen, a shift of 17 mV in equilibrium potential roughly doubles the concentration of Ag^+ above a particle.[17] For small particles, size disparities create a concentration gradient that allows for the diffusion of silver ion toward larger particles. The diffusion time for a silver ion to travel 10 nm in water is 30 ns.[18] A net transfer of Ag^+ ion occurs; this can be described as follows. In step 1 an aqueous silver ion plates out onto the larger nanoparticle by accepting an electron. To reestablish electrical equilibrium, the larger nanoparticle accepts an electron from a neighboring smaller particle through the conducting substrate. The smaller, now even more positively charged nanoparticle reestablishes equilibrium by dissolving an Ag^+ ion into solution. Silver ion thus acts as a reaction initiator, as is observed experimentally. The pure silver film does not react without some initial oxidized component, and the addition of silver nitrate increases the rate. The potential difference between the larger and smaller particles increases as the reaction proceeds. Once the particles become larger and smaller particles are no longer present, differences in equilibrium silver ion concentration and electrostatic charge cannot provide a driving force significant enough for the reformation to continue.

This mechanism requires the standard electrode potential of the Ag particles to be established by physical size, and not affected by the conductive substrate. There must be weak tunneling electron transfer between particles and substrate; Penner has previously established this weak coupling limit for Ag particles on HOPG electrodes in aqueous cells.[19]

It is interesting, within the theoretical framework of Plieth, that films as thick as 60 nm reform. According to eq 1, the standard electrode potential of a 60 nm particle is shifted 4 mV from that of a 65 nm particle. Equation 1 is valid for perfect crystals. The growing faceted particles (see Figures 1F, 2C, 4B) are presumed to be single crystals while the initial evaporated film is polycrystalline. It has been shown that the standard exchange rate of $Ag^+_{(aq)} + e^- \leftrightarrow Ag^0_{(surface)}$ at polycrystalline electrodes is 3−4 orders of magnitude faster than at bulk-terminated Ag(100) surfaces.[1] Thus the

system is kinetically and thermodynamically biased toward the formation of larger single crystals.

The reaction slows in an inert salt solution ($NaNO_3$), which can serve to screen the solution electric field causing transport of Ag^+ ions to the larger particles. Citrate ion also inhibits reformation. Citrate is widely used as a reducing agent in the formation of metallic nanoparticles;[20−22] citrate-coated particles are thought to not have surface oxide. In the absence of citrate, the solubility of Ag metal should be pH dependent:

$$4Ag + O_2 + 4H^+ \rightarrow 4Ag^+ + 2H_2O \qquad (2)$$

In agreement with this, we found that acidic solutions speed reformation while basic solutions inhibit it.

This Ostwald electrochemical mechanism may be involved in other experiments. Mirkin et al. reported the formation of Au−Ag cubes when a 45 nm thick evaporated silver film, deposited on a 1 nm thick Ti adhesion layer on quartz, was exposed to various aqueous solutions.[23] They concluded that an unknown process was forming the cubes. We suggest that the insoluble titanium layer serves as a conductive substrate, thus setting up the conditions necessary for Ostwald electrochemical growth.

Murakoshi et al. found that *continuous* silver films sputtered on glass will reform when exposed to an external electric field and irradiated with light on the order of 1 mW/cm^2 in aqueous solution.[24,25] In their experiment, the touching particles perform the same role as a conducting substrate. The reformation then halts when the particles no longer touch. Murakoshi et al. noted that while continuous films reformed, films with discrete islands did not. It is possible that electrochemical reformation affected their results.

Penner et al. carried out careful studies of the reductive nucleation, growth and coarsening of Ag nanoparticles on HOPG electrodes under voltage control.[18,26] Much of their growth data is explained by "interparticle diffusion coupling" in which the Ag^+ depletion regions around each growing particle interact with each other. Yet they concluded that other unknown processes must be involved to explain the observation that particle size distributions did not narrow with increasing growth time. In Ostwald electrochemical coarsening, the larger particles scavenge smaller ones, broadening the size distribution with time. We suggest that Ostwald electrochemical coarsening occurred in their experiment.

This paper demonstrates the sensitivity of the electrochemical properties of metallic nanostructures at remarkably large sizes (∼50 nm). This result will affect bare metallic nanostructures on conducting substrates,[27−30] even in the absence of water. Variability in size will cause differences in the electrostatic charge on each structure at electrical equilibrium.[31] In water, electrochemical Ostwald ripening allows for size control through the variation of solution pH, salt concentration, and the electric potential of the conducting surface. Importantly, the reformation can be shut off by the addition of a stabilizing agent such as citrate.

Acknowledgment. We thank Mathieu Maillard, Erich Walter, and Michael Steigerwald for valuable discussions and comments. This work has been supported by DOE Basic Energy Sciences under FG02-98ER14861, by the AFOSR MURI program, and by the NSF Nanocenter at Columbia under CHE-010110655. We have used characterization facilities supported in part by the NSF MRSEC Program under DMR-0213574 and by the New York State Office of Science, Technology and Academic Research (NYSTAR).

Supporting Information Available: Experimental setup, SEM images, and UV−vis images of reforming films. This material is available free of charge via the Internet at http://pubs.acs.org.

References

(1) Porter, J. D.; Robinson, T. O. *J. Phys. Chem.* **1993**, *97*(25), 6696−6709.
(2) Henglein, A. *J. Phys. Chem.* **1993**, *97*(21), 5457−54571.
(3) Plieth, W. J. *J. Phys. Chem.* **1982**, *86*(16), 3166−3172.
(4) Plieth, W. *J. Surf. Sci.* **1985**, *156*, 530−535. In this paper eq 6b gives the change in the work function with decreasing size. Unlike eq 1 above for the standard electrode potential, the work function equation has two terms which vary with size. The first is a negative shift dependent upon surface energy as in eq 1. The second term is a charging energy term, which gives a positive shift for smaller sizes. In a vacuum smaller Ag particles would have larger ionization potentials than bulk Ag − the second term dominates numerically. In water, dielectric screening makes the second term negligible with respect to the first. Smaller Ag particles would have lower ionization potentials than bulk Ag. Also note that in Plieth's equation 6b the charging energy term has a numerical factor of 3/8. It is now thought that this factor should be 1/2: see Makov, G.; Nitzan, A.; Brus, L. *J. Chem. Phys.* **1988**, *88*, 5076.
(5) Michaels, A. M.; Nirmal, M.; Brus, L. E. *J. Am. Chem. Soc.* **1999**, *121*(43), 9932−9939.
(6) Nie, S.; Emory, S. R. *Science* **1997**, *275*, 1102−1106.
(7) Kneipp, K.; Wang, Y.; Kneipp, J.; Perelman, L. T.; Itzkan, I.; Dasari, R.; Reld, M. S. *Phys. Rev. Lett.* **1997**, *78*, 1667.
(8) Xu, H. X.; Bjerneld, E. J.; Kall, M.; Borjesson, L. *Phys. Rev. Lett.* **1999**, *83*, 4357.
(9) Weiss, A.; Haran, G. J. *Phys. Chem. B* **2001**, *105*, 12348.
(10) Kamat, P. V. *J. Phys. Chem. B* **2002**, *106*(32), 7729−7744.
(11) Cai, W.; Zhong, H.; Zhang, L. *J. Appl. Phys.* **1998**, *83*(3), 1705−1710.
(12) Schmidt, M.; Masson, A.; Brechignac, C. *Phys. Rev. Lett.* **2003**, *91*(24), 243401.
(13) Jiang, Q.; Liang, L. H.; Zhao, D. S. *J. Phys Chem. B* **2001**, *105*(27), 6275−6277.
(14) Ng, K. H.; Liu, H.; Penner, R. M. *Langmuir* **2000**, *16*(8), 4016−4023.
(15) Chaki, N. K.; Sharma, J.; Mandle, A. B.; Mulla, I. S.; Pasricha, R.; Vijayamohanan, K. *Phys. Chem. Chem. Phys.* **2004**, *6*(6), 1304−1309.
(16) Bockris, J. O'M.; Reddy, A. *Modern Electrochemistry*; Plenum: New York, 1970; p 1267.
(17) Alberty, R. A.; Silbey, R. J. *Physical Chemistry*, 2nd ed.; John Wiley & Sons: New York, 1996; eq 7.44, p 227.
(18) Albright, J. G.; Miller, D. G. *J. Phys. Chem.* **1972**, *76*(13), 1853−1857.
(19) Penner, R. M. *J. Phys. Chem. B* **2002**, *106*(13), 3339−3353.
(20) Enustun, B. V.; Turkevich, J. *J. Am. Chem. Soc.* **1963**, *85*(21), 3317−3328.
(21) Lee, P. C.; Meisel, D. J. *J. Phys. Chem.* **1982**, *86*(17), 3391−3395.
(22) Henglein, A.; Giersig, M. *J. Phys. Chem. B* **1999**, *103*(44), 9533−9539.
(23) Zhang, H.; Jin, R.; Mirkin, C. A. *Nano Lett* **2004**, *4*(8), 1493−1495.
(24) Murakoshi, K.; Tanaka, H.; Sawai, Y.; Nakato, Y. *J. Phys. Chem. B* **2002**, *106*(12), 3041−3045.
(25) Murakoshi, K.; Tanaka, H.; Sawai, Y.; Nakato, Y. *Surf. Sci.* **2003**, *532−535*, 1109−1115.
(26) Liu, H.; Penner, R. M. *J. Phys. Chem. B* **2000**, *104*(39), 9131−9139.
(27) Gunnarsson, L.; Bjerneld, E. J.; Xu, H.; Petronis, S.; Kasemo, B.; Kall, M. *App. Phys. Lett.* **2001**, *78*(6), 802−804.

(28) Schilder, G.; Krenn, J. R.; Hohenau, A.; Ditlbacher, H.; Leitner, A.; Aussenegg, F. R.; Schaich, W. L.; Puscasu, W. L.; Monacelli, B.; Boreman, B. *Phys. Rev. B* **2003**, *68*, 155427.
(29) Fromm, D. P.; Sundaramurthy, A.; Schuck, P. J.; Kino, G.; Moerner, W. E. *Nano Lett*. **2004**, *4*(5), 957−961.
(30) Zhang, H.; Mirkin, C. A. *Chem. Mater*. **2004**, *16*(8), 1480−1484.
(31) Note here the discussion in ref 3.

NL048204R